

# Characteristic Spike-and-Wave Discharges Link Dystonic Attack Progression and Absence Seizures in EA2 Mouse Model Tottering

Anant Naik<sup>1</sup>, Russell Carter, Ph.D.<sup>2</sup>, Madelyn Gray<sup>2</sup>, Timothy Ebner, M.D./ Ph.D.<sup>2</sup>

<sup>1</sup>Department of Biomedical Engineering, <sup>2</sup>Department of Neuroscience, University of Minnesota Twin Cities



## INTRODUCTION AND BACKGROUND

Episodic Ataxia Type II (EA2) is a rare, debilitating neurological disease caused by a mutation in the human *CACNA1A* gene encoding the P/Q-type voltage-gated  $Ca^{2+}$  channel. As  $Ca^{2+}$  is vital for neurotransmitter release (1), a process governing nearly all neuronal interactions, EA2 has a very complex prognosis. Clinically, the occurrence of transient episodes of severe ataxia and dystonia has predominantly been attributed to dysfunction of the cerebellum, whereas symptoms like absence seizures and headaches have been attributed to various cerebral regions of the brain (2,3).

The most prominent of the phenotypes present in the *tg/tg* mouse model is the presence of episodic full-body dystonic attacks. Previous experiments have shown that these attacks can also be induced pharmacologically with caffeine, and other stressful (8). Though the general progression of this dystonia has been described, we sought to elaborate on the specific changes over time during the dystonic attack.

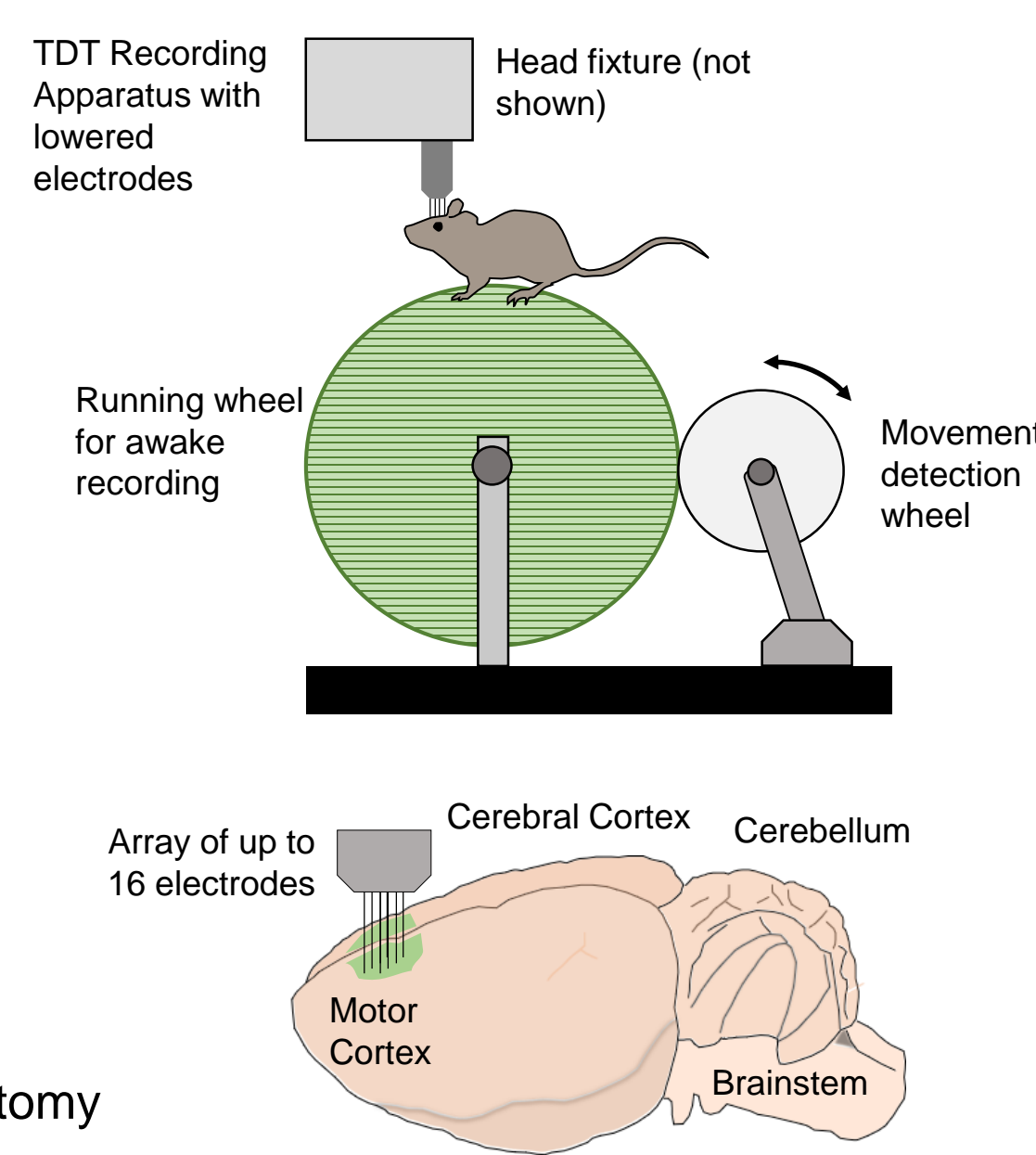
It was recently found that high-power low-frequency oscillations occurred in the motor cortex of anesthetized *tg/tg* mice (7). However, little is known about the role about the motor cortex has in the dystonic attack progression. Previous literature utilizing methods such as EEG and ECoG recordings have shown absence seizures, a symptom of EA2, to be correlated to spike-and-wave discharges (SWDs) in the motor cortex of *tg/tg* mice (5,6), yet their role in attack progression is not clear.

In this set of experiments, we sought to investigate if the neuronal activity in the motor cortex changes before the attack, after the induction of a dystonic attack, and during the recovery post-attack. We utilized local field potential recordings (LFP) from the motor cortex in awake head-fixed *tg/tg* mice to see if we could determine neuronal changes that would help us understand the dystonic attack progression.

## METHODS

### Behavior Experiments

- 3+ months old *tg/tg* or littermate controls were tested.
- Mice were exposed to three treatments after removal from home cage:
  - 75  $\mu$ L of 2 mg/mL caffeine (IP) and new cage transfer
  - 75  $\mu$ L of saline (IP) and new cage transfer
  - Only new cage transfer.
- The resulting dystonic attack was scored on two scoring systems (0 – 3 for a full body attack and 0 – 1 for regional contraction) every five minutes for the duration of the attack with  $t = 0$  at the start of injection.



### Chamber Implant for Awake Recordings

- *tg/tg* mice were anesthetized, and a craniotomy was drilled into the motor cortex.
- 3D-printed guide chambers were implanted over the craniotomy and affixed to the skull with dental cement and sealed with Kwik-Sil.
- Sterile agarose gel and saline were placed into chamber for recovery period.
- Mice were allowed to recover for 3-4 days to allow for healing and accommodation prior to training.
- Mice were gradually acclimated to head fixture and recording apparatus over 3 days prior to electrophysiological recording.

### Electrophysiological Recording

- Mice were head fixed on apparatus, and a multi-electrode array (TDT) used to lower up to 16 electrodes through the guide port in the chamber implant.
- Electrodes were lowered into the brain until consistent cells were obtained, and their z-location recorded.

### Data Analysis

- Data analysis was conducted in MATLAB and GraphPad Prism. Analysis between animals was conducted on individual channels after verification that individual channels within each recording set were highly correlated using standard cross-correlation algorithms. Upon verification, the channel best representative of the overall signal was selected.

## BEHAVIORAL PROGRESSION OF THE DYSTONIC ATTACK

Score	Characteristics
0	Full mobility of mouse, no visible contractions
1	Partial loss of mobility with minimal contractions, stillness without excessive contractions
2	Limited capacity for movement, abnormal posture, Tripod position with prominent contractions
3	Immobility, ipsilateral contractions, rolling on belly and curling, prolonged contractions

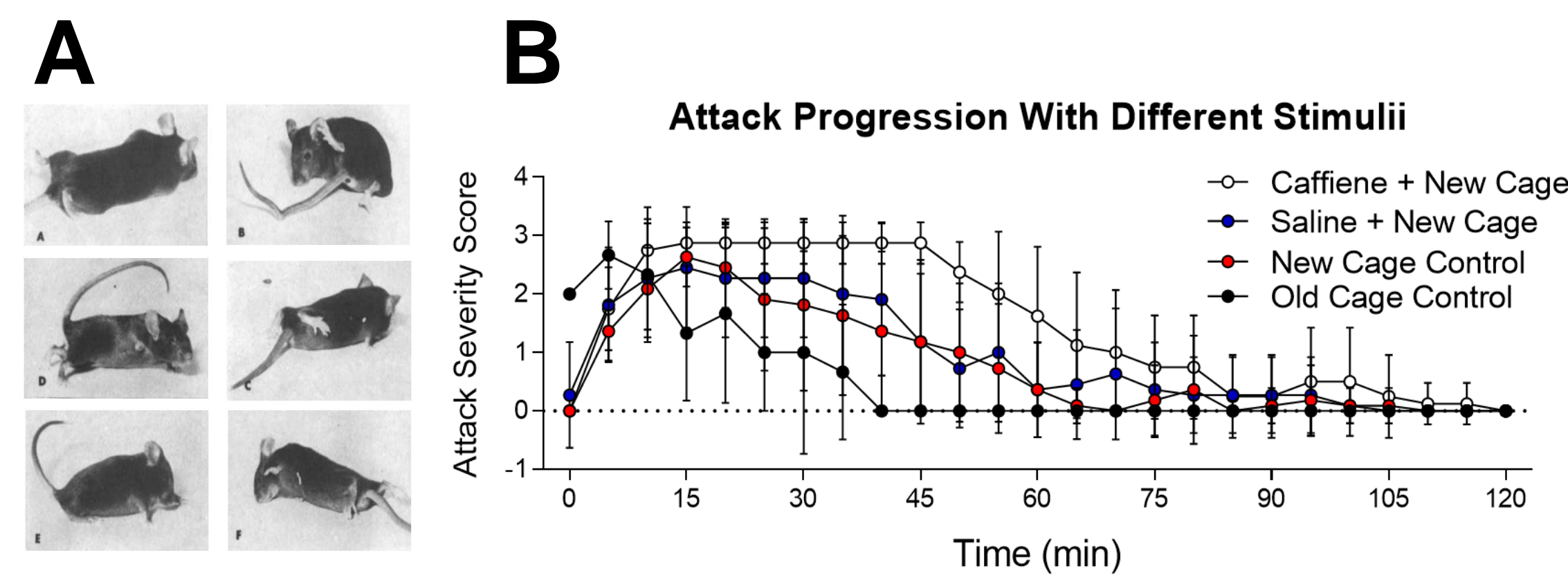


**Figure 1.** A scale constructed to measure the severity of the attack observed over time. The scale was used to monitor the severity of the attack in **B**. **A**. Series of images showing the progress of the attack (from Green and Sidman, 1962). **B**. Summary data comparing the attack severity and duration between caffeine, saline, or new cage animals (n=10 each). Caffeine injected animals were significantly different than saline and new cage animals (ANOVA  $F(2,747)=17.99$ ,  $p<.0001$ ).

## CHARACTERISTICS OF THE SPIKE AND WAVE DISCHARGES (SWDs)

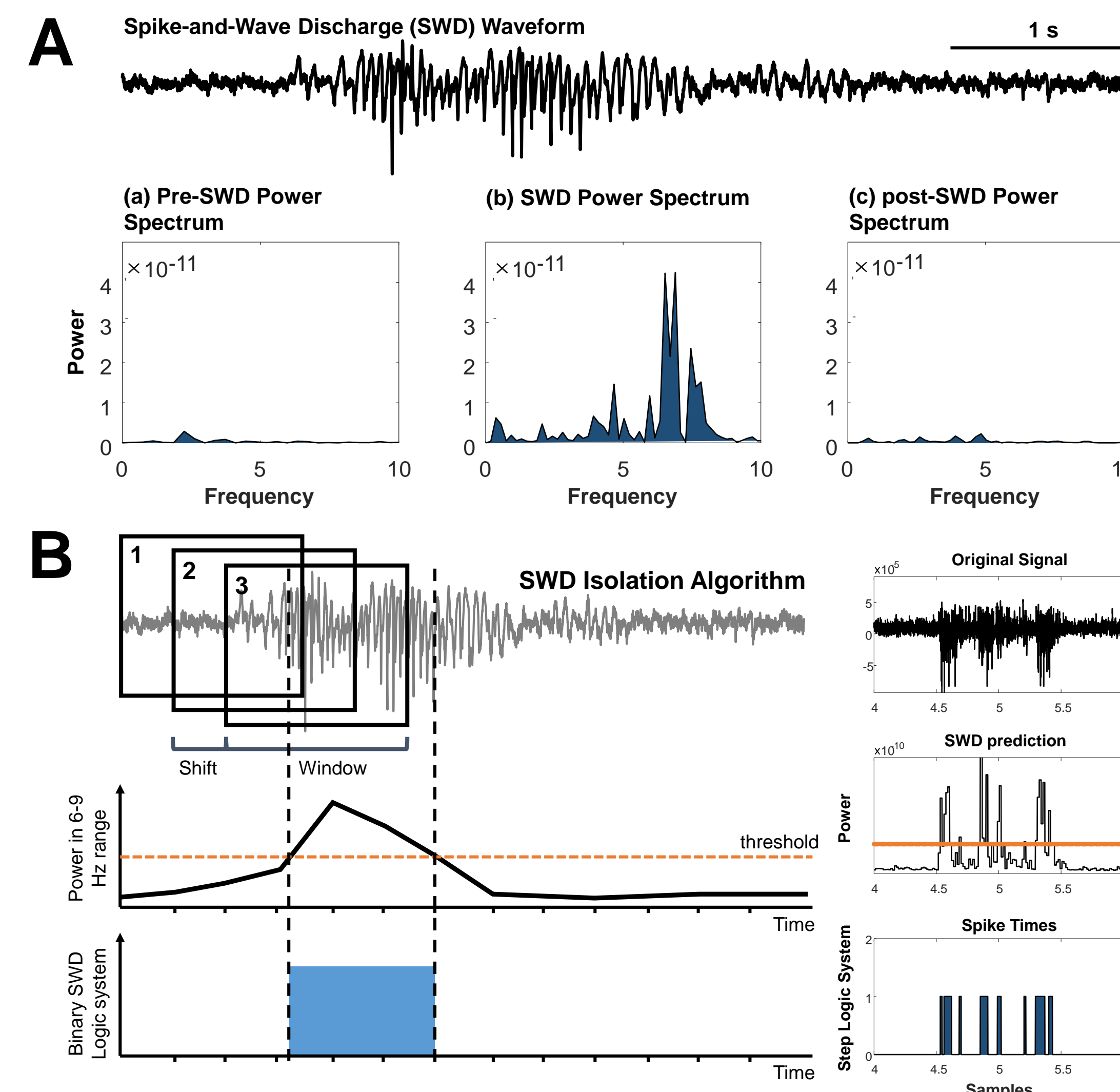


**Figure 2.** The characterization of spike-and-wave discharges (SWDs) in the LFP signal from the motor cortex. **A**. A sample trace from a recording is shown. A very low power noise oscillates in this region. Eventually, on the sample trace, more prominent waveforms are evident until the SWD is prominent. For the duration of the SWD, high power oscillations in the 6-9 Hz band are distinctly observed. These oscillations in this band of interest (BOI) return to pre-SWD levels. Prior to the suppression of the SWD waveforms, lagging waves remain. **B**. A novel method described to isolate the time points at which SWDs occur. Using the BOI determined in **A**, the power spectrum is windowed with a time shift. As the window moves, the power spectrum is calculated, and the maximum power in the BOI is tabulated. The tabulation of power is then thresholded manually to optimize minimal isolation of non-SWD discharges. The threshold is used to construct a logic binary signal, which is differentiated to obtain the start points. Upon differentiation, the positive values are the time points at which the SWD is determined to start.

## SWD RELATION TO DYSTONIC ATTACK

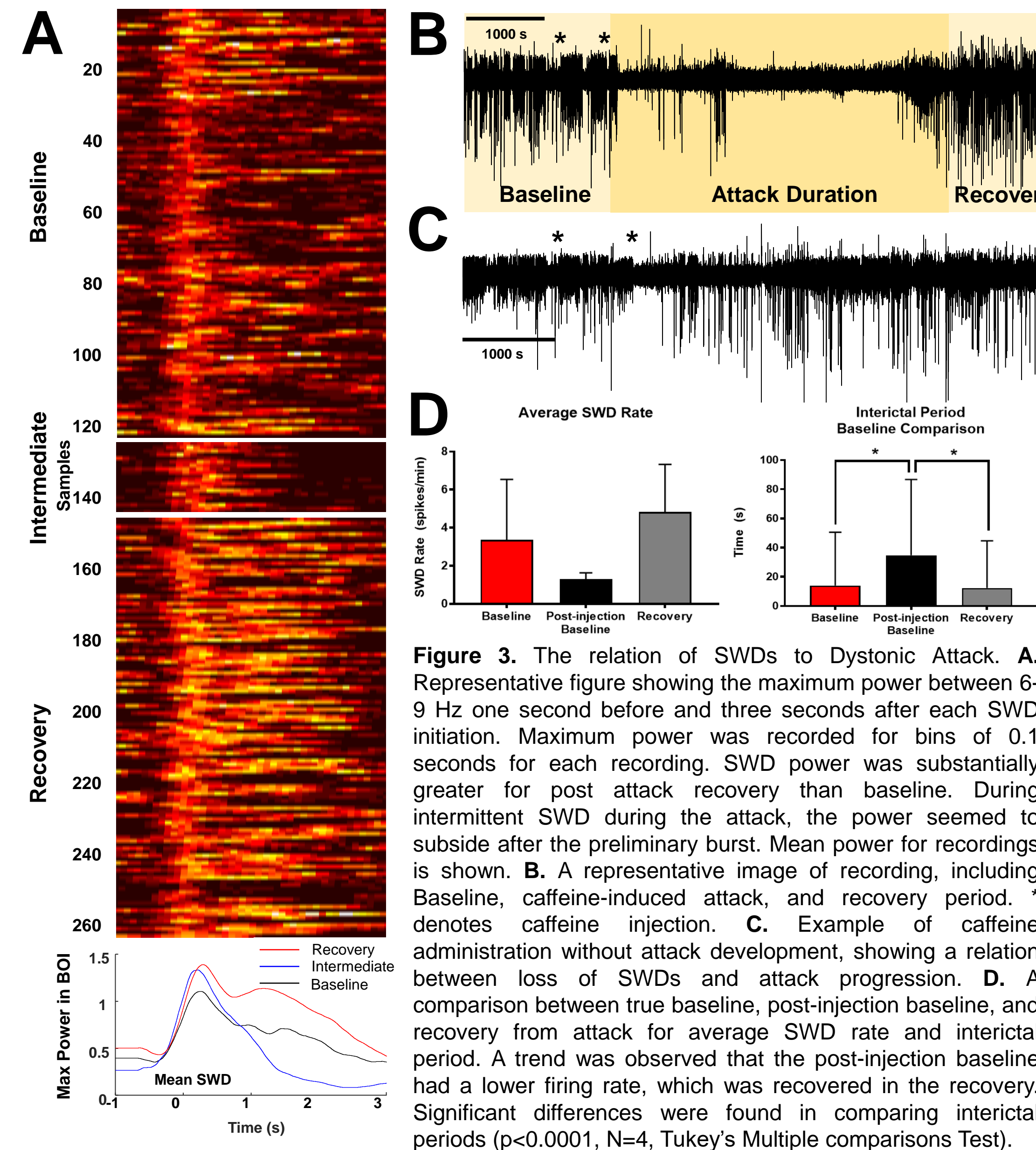


**Figure 3.** The relation of SWDs to Dystonic Attack. **A**. Representative figure showing the maximum power between 6-9 Hz one second before and three seconds after each SWD initiation. Maximum power was recorded for bins of 0.1 seconds for each recording. SWD power was substantially greater for post attack recovery than baseline. During intermittent SWD during the attack, the power seemed to subside after the preliminary burst. Mean power for recordings is shown. **B**. A representative image of recording, including Baseline, caffeine-induced attack, and recovery period. \* denotes caffeine injection. **C**. Example of caffeine administration without attack development, showing a relation between loss of SWDs and attack progression. **D**. A comparison between true baseline, post-injection baseline, and recovery from attack for average SWD rate and interictal period. A trend was observed that the post-injection baseline had a lower firing rate, which was recovered in the recovery. Significant differences were found in comparing interictal periods ( $p<0.0001$ ,  $N=4$ , Tukey's Multiple Comparisons Test).

## SWD LINK TO ABSENCE SEIZURES

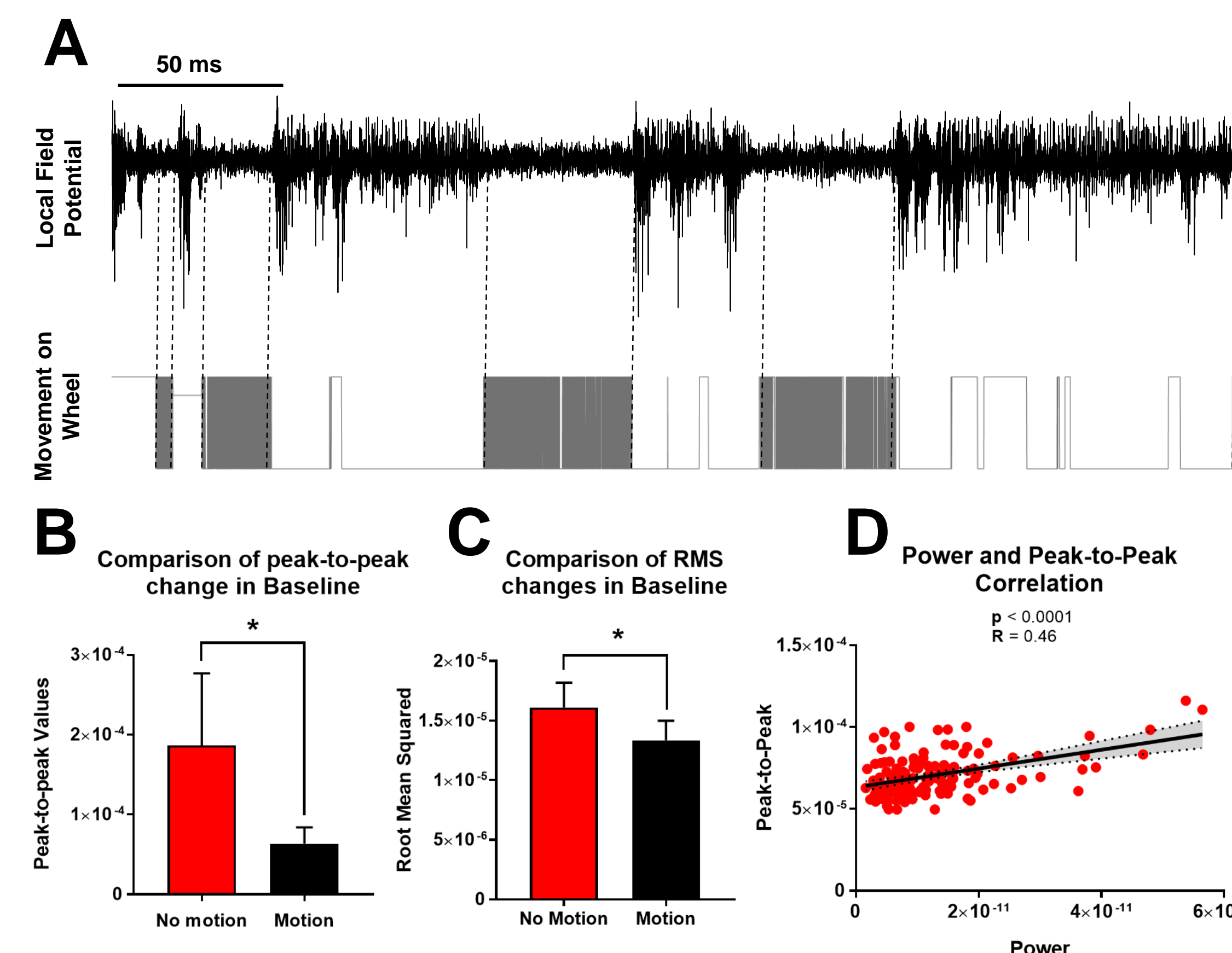


**Figure 4.** Elucidating the link between absence seizures and SWDs. **A**. Representative figure from an active channel during a baseline recording showing LFP activity and wheel movement. **B**. For all baseline recordings, the data was segmented into movement and no-movement. Peak-to-peak values over a 2 second bin was observed and compared between two groups. SWD activity during the *no motion* phase shows a higher peak-to-peak range than motion ( $n = 3$ , Two-tailed Mann-Whitney Test,  $p < 0.0001$ ). **C**. For all base, data was segmented analogously to **B**, and RMS values were found to be statistically significant ( $n = 3$ , Two-tailed Mann-Whitney Test,  $p < 0.0001$ ). **D**. Previous results showed that SWDs were high power events. To show that Peak-to-peak measures were valid measures, the maximum power in the 6-9 Hz range was used to validate the parameter ( $R = 0.46$ ,  $p < 0.0001$ ).

## FUTURE DIRECTIONS

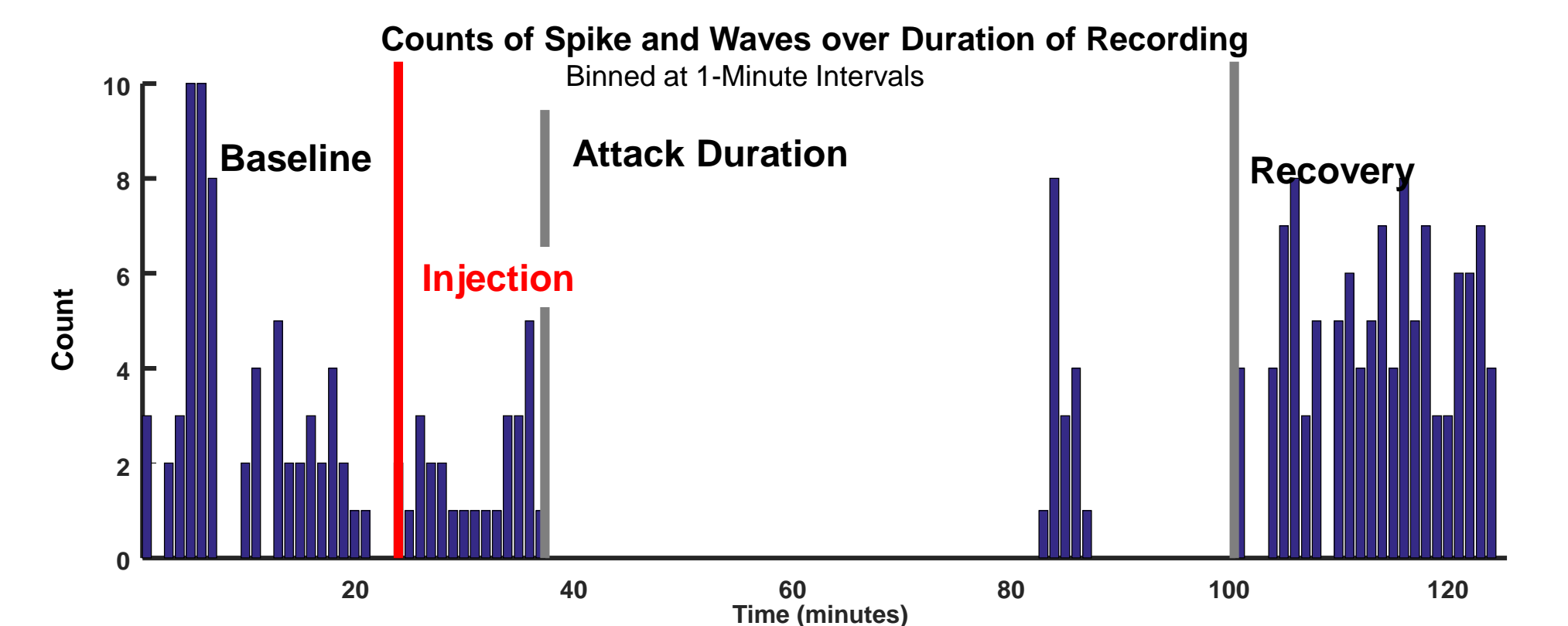


**Figure 5.** Representative figure for SWDs/minute over duration of recording. First injection of caffeine occurred at 25 minutes. Following injection, SWD rate transiently increased leading into attack before complete abolishment. SWD rate was more prominent in recovery.

- Future experiments must also record the attack progression using scale developed to correlate attack severity to electrophysiological observations made in LFP signal.
- Simultaneous recordings of electrophysiological LFP and flavoprotein Autofluorescence imaging in awake mice can elucidate the relation of broad spectrum activity in regions of interest to region-specific signal observed. Dystonic attack scoring would also be used to correlate and time-peg behavioral progression and important physiological activity to the behavioral changes observed in *tg/tg* mouse experiments.

## DISCUSSION

In head-fixed *tg/tg* mice, LFP data was acquired and analyzed during caffeine induced attacks. Changes were observed in neural activity before induction, after injection, during dystonic attack, and recovery.

- The dystonic attack follows a distinct attack progression.
- SWD waveforms followed a characteristic spectral density over time
  - High power observed in a 6-9 Hz band of interest during the SWD
- SWD properties changed over the course of the attack
  - Recovery waveforms were longer and more higher power than baseline.
  - Changes in the average rate and the inter-ictal period between baseline/recovery and immediately following injection.
- Correlation between SWD activity and movement
  - Peak-to-peak measurements in regions of motion compared to no motion confirms previous findings.

## REFERENCES

1. Ayata C et al. (2000) Impaired neurotransmitter release and elevated threshold for cortical spreading depression in mice with mutations in the alpha1A subunit of P/Q type calcium channels. *Neuroscience* 95(3):639-45
2. Nachbauer W et al. (2014) Episodic Ataxia Type 2: Phenotype Characteristics of a Novel *CACNA1A* mutation and Review of the Literature. *J Neuro* 261:983-991
3. Wapfl E et al. (2002) Functional Consequences of P/Q-type  $Ca^{2+}$  Channel Cav2.1 Missense Mutation Associated with Episodic Ataxia Type 2 and Progressive Ataxia. *Jour. of Biol Chem* 277(9):6960-6966
4. Green MC, Sidman RL (1962) Tottering - A Neuromuscular Mutation in the Mouse and its Linkage with Oligosyndactylism. *J Hered* 53:233-7
5. Kaplan BJ, et al. (1979) Spontaneous Polyspike Discharges in an Epileptic Mutant Mouse (Tottering). *Exp Neurol* 66: 577-586.
6. Kros L et al. (2015) Cerebellar Output Controls General Spike-and-Wave Discharge Occurrences. *Annals of Neuro*. 77(6):1027-49.
7. Cramer SW et al. (2015) Abnormal excitability and episodic low frequency oscillations in the cerebral cortex of the tottering mouse. *J Neurosci* 35(14):5664-79.
8. Raiké RS et al (2013) Stress, caffeine and ethanol trigger transient neurological dysfunction through shared mechanisms in a mouse calcium channelopathy *Neurobiology of Disease*: 50:151-159.

## ACKNOWLEDGEMENTS

This work was supported by the resources of Dr. Ebner's Lab (Grants: T32 G M008244, T32 GM008471, P30 NS062158, and R 01 NS18338) and funded partly by the Undergraduate Research Opportunities Program.